ACS Sustainable Chemistry & Engineering

Research Article

pubs.acs.org/journal/ascecg

Room-Temperature Electrocatalytic Synthesis of NH_3 from H_2O and N_2 in a Gas–Liquid–Solid Three-Phase Reactor

Shiming Chen,*[,†,‡] Siglinda Perathoner,*[,†] Claudio Ampelli,[†] Chalachew Mebrahtu,[†,‡] Dangsheng Su,[§] and Gabriele Centi[†]

[†]Departments of MIFT and ChiBioFarAM (Industrial Chemistry), University of Messina, ERIC aisbl and INSTM/CASPE, V.le F. Stagno D'Alcontres 31, Messina 98166, Italy

[‡]Lehrstuhl für Heterogene Katalyse und Technische Chemie, Institut für Technische und Makromolekulare Chemie (ITMC) RWTH Aachen University, Worringerweg 2, Aachen 52074, Germany

[§]Dalian Institute of Chemical Physics, Chinese Academy of Sciences, 457 Zhongshan Road, Dalian 116023, China

ABSTRACT: Fe_2O_3-CNT samples are studied for the room-temperature electrocatalytic synthesis of NH_3 from H_2O and N_2 in a gas–liquid–solid three-phase reactor. A 30 wt % iron-oxide loading was found to be optimal. The performances greatly depend on the cell design, where the possibility of ammonia crossover through the membrane has to be inhibited. The reaction conditions also play a significant role. The effect of electrolyte (type, pH, concentration) was investigated in terms of current density, rate of ammonia formation, and Faradaic efficiency in continuous tests up to 24 h of time on stream. A complex effect of the applied voltage was observed. An excellent stability was found for an applied voltage of −1.0 V vs Ag/AgCl. At higher negative applied voltages, the ammonia formation rate and Faradaic selectivity are higher, but with a change of the catalytic performances, although the current densities remain constant for at least 24 h. This effect is interpreted in terms of reduction of the iron-oxide species above a negative voltage threshold, which enhances the side reaction of H^+/e^- recombination to generate H_2 rather than their use to reduce activated N_2 species, possibly located at the interface between iron-oxide and functionalized CNTs.

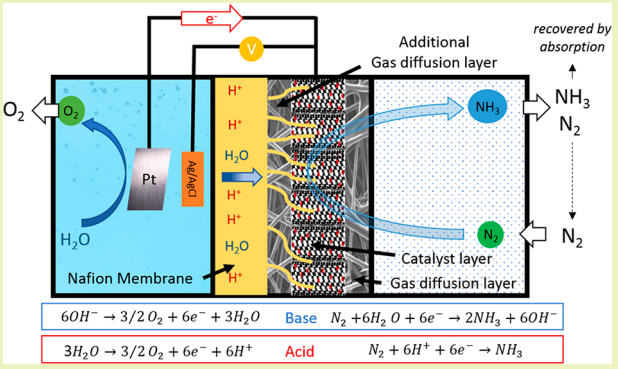

KEYWORDS: *N_2 activation, NH_3 synthesis, Electrocatalysis, Fe/CNT, Electrocatalytic reactor*

INTRODUCTION

A major challenge facing chemistry to move to a sustainable, low-carbon future is to avoid the need of using fossil fuels to supply the energy to drive the processes, which accounts for the largest part of carbon oxides emissions. A major current effort is thus to develop novel synthetic paths using directly renewable energy (RE) sources to drive industrial processes.[1] With ammonia being the largest-scale chemical (>150 Mtons y^{-1}) with the top largest chemical process in terms of energy consumption (about 2.5 EJ on a world scale), it is not surprising the fast emerging interest to develop new solutions to synthesize NH_3 from N_2 using RE as energy source for the process.[2] Between the various solutions under development, the electrocatalytic conversion of N_2 is one of the most attractive, and one of the challenging directions is the possibility of N_2 and H_2O coelectrolysis in very mild conditions, around room temperature and atmospheric pressure.[2−7] This solution offers also attractive possibilities for a distributed production of fertilizers.[2]

While initial studies on the ammonia electrosynthesis from N_2 at temperatures below 100 °C with in situ generation of the H_2 (or H^+/e^- equivalents) from H_2O were based on the use of noble-metal supported catalysts,[8,9] we reported recently that iron nanoparticles supported on carbon nanotubes (Fe/CNT) are effective and stable electrocatalysts in this process.[10] The use of electrocatalysts not containing noble metals is a relevant target to avoid the use of critical raw materials and thus further enhance the sustainability of the novel process.

A general issue present in the literature on the ammonia electrosynthesis from N_2 in mild reaction conditions is that the efficiency of the process greatly depends on the type and configuration of the electrocatalytic reactor and reaction conditions, besides that from the electrocatalyst, although there are often not clear indications on these aspects. The objective of this work is thus to analyze the optimization both of the Fe/CNT electrocatalyst and of the reactor/reaction conditions, in particular, the pH and nature of the electrolyte, the iron loading and type of iron species supported on CNTs,

Received: June 1, 2017
Revised: July 10, 2017
Published: July 13, 2017

DOI: 10.1021/acssuschemeng.7b01742
ACS Sustainable Chem. Eng. 2017, 5, 7393−7400

and membrane-assembly in the electrocatalytic reactor. A relevant aspect to remark, in fact, is that to improve the scalability and applicability of the results, it is necessary to utilize an electrocatalytic reactor design different from the conventional electrocatalytic cells and closer to the design in proton exchange membrane (PEM)-type fuel cells, where gas-diffusion electrodes on both sides of the proton-conductive membrane are used. This compact design allows a faster scale-up and additional advantages, as remarked for photoelectro catalytic (PEC) cells.[11] However, this design influences also the performances and characteristics of the electrodes to develop. Specifically, we will discuss here how to optimize both the electrocatalysts and the reactor/reaction conditions used in the early report,[10] where a nonconventional electrocatalytic cell was used. This cell is characterized by a membrane-electrode assembly separating the two parts of the cell, the first containing a diluted aqueous solution for water electrolysis to generate the protons and electrons used in the other hemicell, where N_2 electrocatalytic conversion to NH_3 is realized in a gas-phase type flow electrocatalytic hemicell. This configuration allows an easy recovery of ammonia from the flow cell.

MATERIALS AND METHODS

Materials and Chemicals. Pyrograph-III, CNT PR-24XT were used as carbon nanotubes (CNTs). A commercial gas diffusion layer (SIGRACET GDL 29BC) supplied by SGL Group and Nafion115 membrane (Sigma-Aldrich) were used to prepare the electrode. Nafion solution (10 wt %) was used to prepare the catalyst ink. Iron(III) nitrate nonahydrate (Sigma-Aldrich, 99.9% purity) was used as precursor during the Fe_2O_3-CNT synthesis. Commercial Fe(III)oxide nanoparticle (<30 nm average particle size) was also used as electrocatalyst for comparison.

Preparation of Electrodes. The preparation of electrodes can be summarized in the following steps.

Step I: Synthesis of Electrocatalysts. Synthesis of the electrocatalysts starts with pretreatment of the commercial CNTs to purify and create surface oxygen functionalities (o-CNT). Briefly, 1 g of CNTs was suspended in 100 mL of concentrated HNO_3 (Sigma-Aldrich, 65%) and treated at 120 °C for 2 h in a reflux setup. The suspension was filtered and washed with DI water until neutral pH. The sample was then dried at 80 °C overnight and ground to obtain homogeneous o-CNT.

Fe_2O_3-CNT Synthesis. 0.5 g of pretreated o-CNT and $Fe(NO_3)_3 \cdot 9H_2O$ (amount was taken with respect to loading %) was dissolved in 25 mL of DI water with 1 mL of ethanol glycol. The mixture was then sonicated for 30 min, and pH was adjusted to 8 with a 5% ammonia solution. After the pH was adjusted, the solvent was eliminated and the sample then dried at 120 °C. The dried sample was then calcined for 2 h at 400 °C in a tubular furnace under He flow. Finally, the obtained sample was ground to get a homogeneous catalyst. Different samples with iron loading in the 6−46% wt range were prepared as reported in Table 1.

Step II: Deposition of the Electrocatalyst on Gas Diffusion Layer (GDL). Ten milligrams of the as-prepared electrocatalyst was suspended in a 5 mL of ethanol and 50 μL of Nafion solution. The solution was sonicated for 90 min to get a homogeneous mixture. Finally, the solution was loaded by spray drying uniformly on the gas diffusion layer (GDL) heated on a hot plate at 100 °C. The GDL with electrocatalyst was stored in an oven at 80 °C overnight.

Step III: Assembling the Electrode. The GDL after depositing the catalyst and a pretreated Nafion membrane was hot pressed together at 80 atm and 130 °C for 30 s. The active composite material was located between these two layers. The membrane electrodes are defined as follows:

Fe_2O_3-CNT. These are membrane electrode assemblies (MEA) with 10 mg of Fe_2O_3-CNT deposited on GDL and hot pressed with the Nafion membrane.

nano-Fe_2O_3. These are MEA with 10 mg of iron-oxide (deposited using commercial Fe(III) oxide nanoparticle dispersion) on GDL and hot pressed with the Nafion membrane.

o-CNT. These are MEA with 10 mg of o-CNT deposited on the GDL and hot pressed with the Nafion membrane.

-blank. These are MEA without catalyst deposited on GDL and hot pressed with the Nafion membrane.

For the improved cell configuration, additional GDL without electrocatalyst was inserted between the catalyst layer and Nafion membrane.

Catalyst Characterization. Atomic absorption spectroscopy (AAS) was used to analyze the iron loading of the as-prepared materials. Catalysts were characterized also by various methods (not reported here), including transmission electron microscopy (TEM) and high-angle annular dark field scanning TEM (HAADF-STEM), X-ray diffraction (XRD), X-ray photoelectron spectroscopy (XPS), and temperature-programmed reduction (TPR) to verify their characteristics and reproducibility.

Testing Conditions. All of the electrochemical measurements were carried out at 20 °C using a potentiostat/galvanostat AMEL 2551. A Pt wire was used as the counter electrode. All of the potentials were measured against Ag/AgCl reference electrode (3 M KCl). A nonconventional type of electrocatalytic cell (operating at atmospheric pressure and room temperature) was developed for these tests, where the solid membrane-electrode assembly separates gas and liquid zones (Figure 1).

The liquid chamber contains a liquid electrolyte for water electrolysis to generate the protons and electrons. The protons and electrons were used in the solid membrane (gas-diffusion) electrode, where the electrocatalytic conversion of N_2 to NH_3 took place. The solid zone consists of a Nafion membrane, catalyst layer, and gas diffusion layer. The reactant N_2 (acting both as reactant and as transport gas for generated ammonia) was continuously fed (20 mL/min of N_2 with purity, 99.9999%), and the flow coming out from the electrocatalytic reactor outlet (containing a mixture of N_2 and ammonia) is sent to a liquid absorber containing a 0.001 M H_2SO_4 solution. The amount of ammonia formed is monitored by a spectrophotometry method. The N_2 may be eventually recycled. The N_2 flow is introduced to the cathode part of the cell 30 min before the start of the reaction and then continuously fed until the end of the test. Further details were described in our previous work.[10]

Table 1. Precursor Amounts of Different Iron Loading Amount Samples[a]

	theoretical iron loading, %	iron loading by AAS, %
5% Fe_2O_3-CNT	6.65	6.16
20% Fe_2O_3-CNT	20.22	18.50
30% Fe_2O_3-CNT	29.55	28.68
45% Fe_2O_3-CNT	46.10	45.25

[a]Weight percentage with respect to the weight of iron oxide (Fe_2O_3).

RESULTS AND DISCUSSION

Effect of Iron Content. The effect of iron oxide loading in Fe_2O_3/CNT electrocatalysts on the performances in NH_3 formation by N_2 and H_2O coelectrolysis at room temperature and atmospheric pressure is summarized in Figure 2. The following membrane-electrode assemblies were tested: without the catalyst (blank) and with 2.5 mg/cm^2 of o-CNT, 5% Fe_2O_3-CNT, 10% Fe_2O_3-CNT, 30% Fe_2O_3-CNT, 45% Fe_2O_3-CNT, and nano-Fe_2O_3 as the electrocatalyst. All of the tests were made using 0.5 M KOH as an electrolyte, with a voltage of −2.0 V vs Ag/AgCl, and a constant flow of 20 mL/min N_2. Figure 2a reports the measured current densities as a function of the time on stream, while Figure 2b summarizes the ammonia formation rate for the various membrane-electrode assemblies.

DOI: 10.1021/acssuschemeng.7b01742
ACS Sustainable Chem. Eng. 2017, 5, 7393−7400

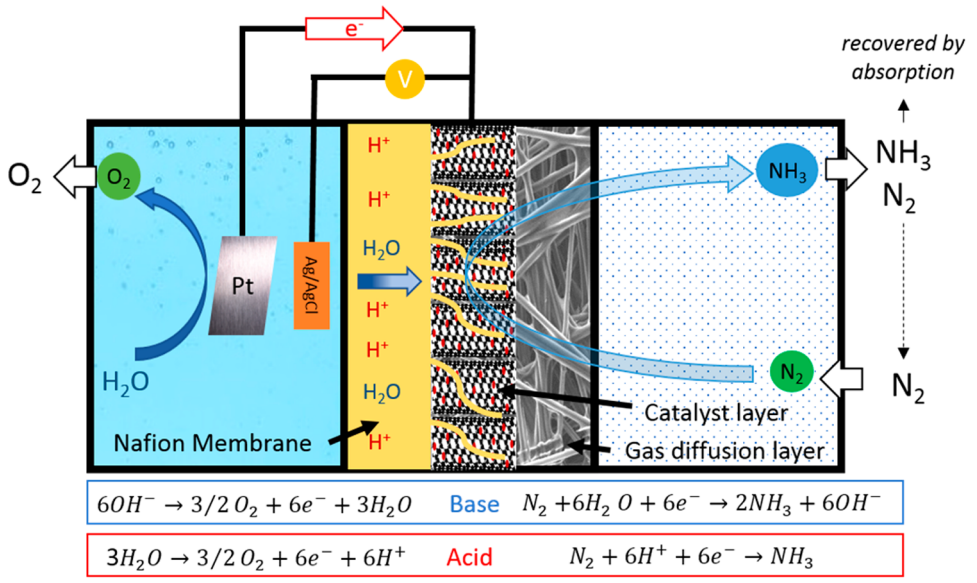

Figure 1. Schematic view of the three-phase reactor for electrochemical ammonia synthesis.

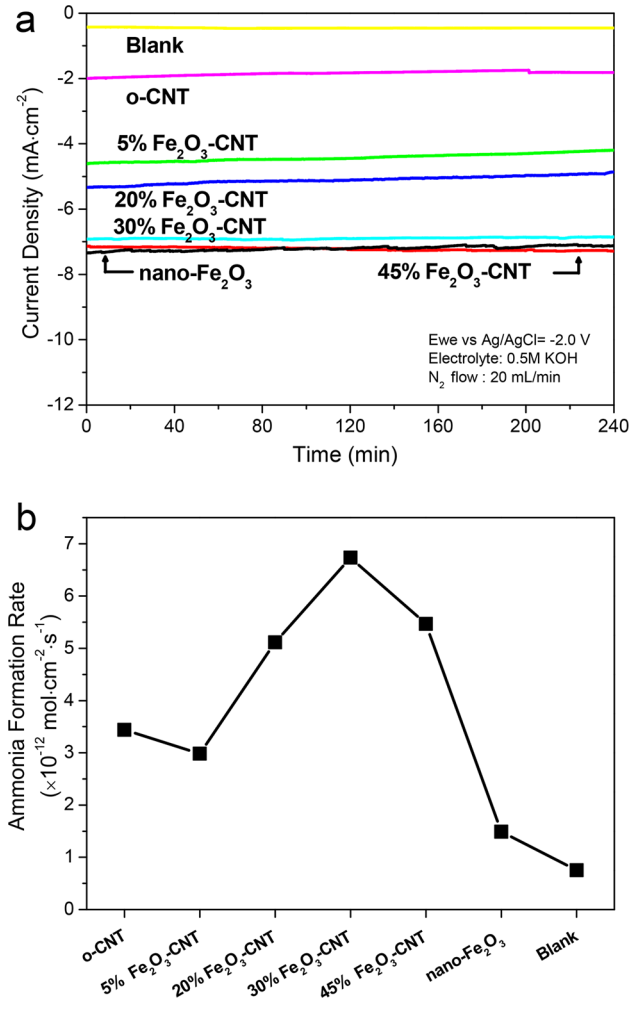

Figure 2. Effect of iron content on (a) current density profile of electrocatalyst, and (b) average ammonia formation rate.

Because the working electrode is used as cathode, the values of current and applied voltage are negative according to the direction of current. In the following discussions, indications to higher or lower values refer thus to the absolute value. The lowest current density (−0.452 mA/cm^2) was shown by the blank sample, while the highest current density (−7.1 mA/cm^2) was shown by nano-Fe_2O_3. Note, however, that this sample, being composed of only iron-oxide rather than iron-oxide loaded on CNTs, contains a higher iron amount. The current density of x-Fe_2O_3-CNT (x = 0, 5%, 20%, 30%, and 45%) increased with increasing iron loading. It is worth pointing out that the current density shown by the sample 45% Fe_2O_3-CNT is almost the same as that shown by nano-Fe_2O_3. This similar behavior indicates that the assumption may be valid that for this high iron-oxide loading, the effect of CNT in modifying the properties of supported iron nanoparticles is minimal. Note that in all cases the current density is stable with time, and thus there are no indications of deactivation or changes in the membrane-electrode assembly. The tests in Figure 2a extend for 4 h, but tests for longer times, up to 50 h of time on stream, showed a similar stable behavior in terms of current density.

The average ammonia formation rates were also measured and reported in Figure 2b. The lowest average ammonia formation rate of 0.75 × 10^{-12} mol cm^{-2} s^{-1} was obtained by the blank sample (carbon paper and Nafion membrane used as working electrode without catalyst). The average of ammonia formation rate shown by o-CNT and nano-Fe_2O_3 was 3.44 × 10^{-12} and 1.49 × 10^{-12} mol cm^{-2} s^{-1}, respectively. These values are lower than the rates obtained by all other x-Fe_2O_3-CNT (x = 0, 5%, 20%, 30%, and 45%) samples. A maximum of ammonia formation rate of 6.74 × 10^{-12} mol cm^{-2} s^{-1} was observed by 30% Fe_2O_3-CNT among all of the samples tested.

Only NH_3 and H_2 were detected during all of the tests. The total Faradaic efficiencies were higher than 90% among all of the electrocatalysts. The Faradaic selectivity to ammonia is 0.028% for the 30% Fe_2O_3-CNT sample showing the best ammonia formation rate (6.74 × 10^{-12} mol cm^{-2} s^{-1}). However, the further experimentation reported below evidences how this value, which is in line with literature data under comparable reaction conditions,[3−5] can be largely improved by optimization of cell design and reaction conditions.

DOI: 10.1021/acssuschemeng.7b01742
ACS Sustainable Chem. Eng. 2017, 5, 7393−7400

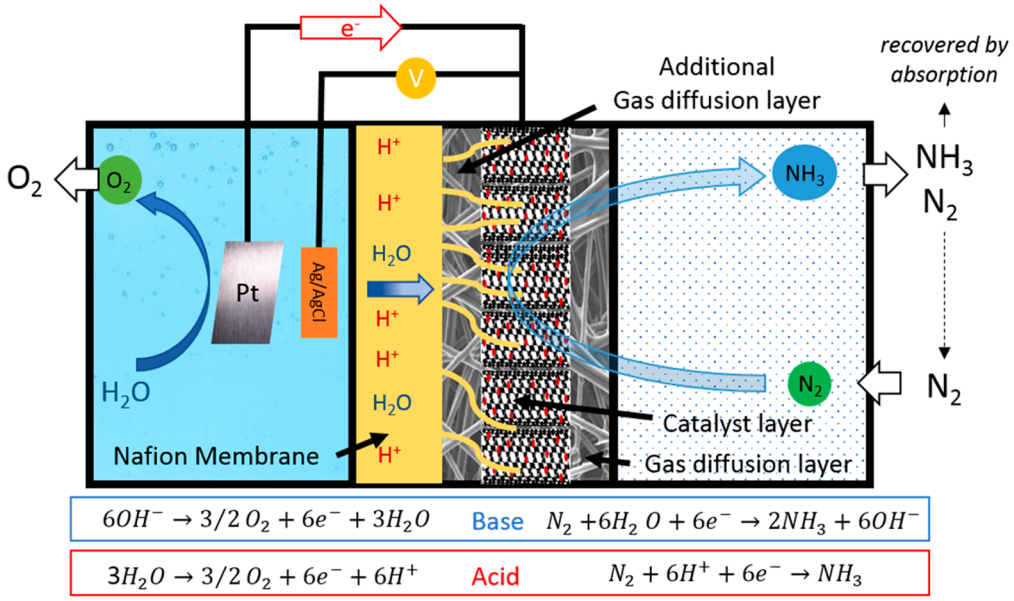

Figure 3. Schematic view of the improved design in the three-phase reactor for electrochemical ammonia synthesis.

Improved Cell Design. A key question in cell design as outlined in Figure 1 is the possible presence of ammonia (or ammonium ion) crossover through the Nafion membrane. Lan et al.[12] observed, in fact, that in a cell using a Nafion membrane as solid electrolyte, ammonia was detected in both the cathode and the anode chambers where oxidation reaction occurred. We have thus analyzed the presence of ammonia in the liquid-phase chamber of the cell shown in Figure 1. The concentration of ammonia in the liquid phase (anode chamber) reaches the highest value after 1 h and then decreases. The explanation of this behavior is that the ammonia formed in the cathodic part passes in part through the membrane (likely in ammonium ion form) and then reacts in the anode chamber according to the following equations:

$$2NH_3 \rightarrow N_2 + 6H^+ + 6e^- \text{ or}$$
$$2NH_3 + 6OH^- \rightarrow N_2 + 3H_2O + 6e^- \quad (1)$$

Part of the ammonia formed is thus consumed according to this mechanism, with a consequent decrease in the efficiency of the process and the rate of ammonia formation. To avoid this negative effect, an additional GDL layer was inserted between the electrocatalyst layer and the Nafion membrane, as shown in Figure 3. This design of the cell strongly decreases the ammonia crossover, and thus the ammonia collection rate increases. However, we have observed that the Faradaic efficiency also increases. By adding a transport layer for protons from the Nafion membrane to the electrocatalyst, we slow the rate of proton arrival to the active sites for the N_2 activation, which is likely the rate-determining step. In this way, it reduced the parallel rate of site H_2 evolution, which depends on the amount of H^+/e^- available. Therefore, the Faradaic efficiency increases. The effect of the electrolyte reported below confirms this interpretation. Note that the proton-transport properties of the additional GDL layer are due to the specific preparation adopted. While in principle the GDL layer should be not able to transport protons, the catalytic layer is added mixed with liquid Nafion, which in part diffuses to the additional GDL layer providing the controlled transport properties of this layer.

An ammonia formation rate of 1.06×10^{-11} mol cm^{-2} s^{-1} with NH_3 Faradaic selectivity of 0.164% was obtained in the modified configuration for the 30% Fe_2O_3-CNT electrocatalyst under the same conditions of previous tests. The ammonia formation rate and NH_3 Faradaic selectivity are therefore 158% and 571% higher than the values acquired with the old configuration (Figure 1). Moreover, no ammonia was detected in the anode part of the new configuration. Different parameters were also optimized using the modified cell configuration reported in Figure 3.

It should be remarked, however, that the additional GDL layer introduced increases the ohmic losses in the half-cell and thus lowers the WE overpotential. This cell design is thus functional to proof the concept that (i) significant ammonia crossover may be present and (ii) the control of the rate of transport of H^+/e^- to the electrocatalytic sites with respect to the rate of N_2 activation is the key to enhance the Faradaic selectivity. This could be realized also in other ways, such as using different proton membranes, operating at higher reaction temperatures, or enhancing the rate of N2 activation by proper electrocatalyst optimization.

Effect of the Electrolyte. The performances of the 30% Fe_2O_3-CNT electrocatalyst were tested in different electrolytes having different pH values, but maintain the applied voltage constant at −2.0 V vs Ag/AgCl. To have data that could be comparable, the electrolytes for these tests were used with different concentrations to have similar liquid-phase conductivity. Specifically, the following values were utilized:

- 0.5 M KOH (pH = 13.7)
- 0.5 M $KHCO_3$ (pH = 9.4)
- 0.25 M K_2SO_4 (pH = 7)
- 0.25 M $KHSO_4$ (pH = 0.6)

Nafion membrane is stable in the pH range explored here at least within our experiments, and we assume that the choice of liquid electrolyte does not impact on the conductivity of the Nafion membrane, in the sense that, as remarked in the previous section, the rate of transport of protons through the membrane is larger than the rate necessary to convert N_2 to NH_3.

DOI: 10.1021/acssuschemeng.7b01742
ACS Sustainable Chem. Eng. 2017, 5, 7393−7400

As shown in Figure 4a, the highest current density of −2.75 mA cm^{-2} was observed for the strong acid 0.25 M $KHSO_4$ (pH = 0.6) electrolyte, while the lowest current density of −1.89 mA cm^{-2} was observed for the basic 0.5 M $KHCO_3$ (pH = 9.4) electrolyte. The neutral electrolyte (0.25 M K_2SO_4; pH = 7) shows an intermediate current density of −2.29 mA cm^{-2}. However, the strongest basic electrolyte (0.5 M KOH, pH = 13.7) shows a current density between those for pH = 7 and pH = 9.4 electrolytes. For a pH above 10, there is thus a deviation in the behavior with respect to the trend expected. This could be explained by considering that both water and proton transport as well as consumption affect the current density.

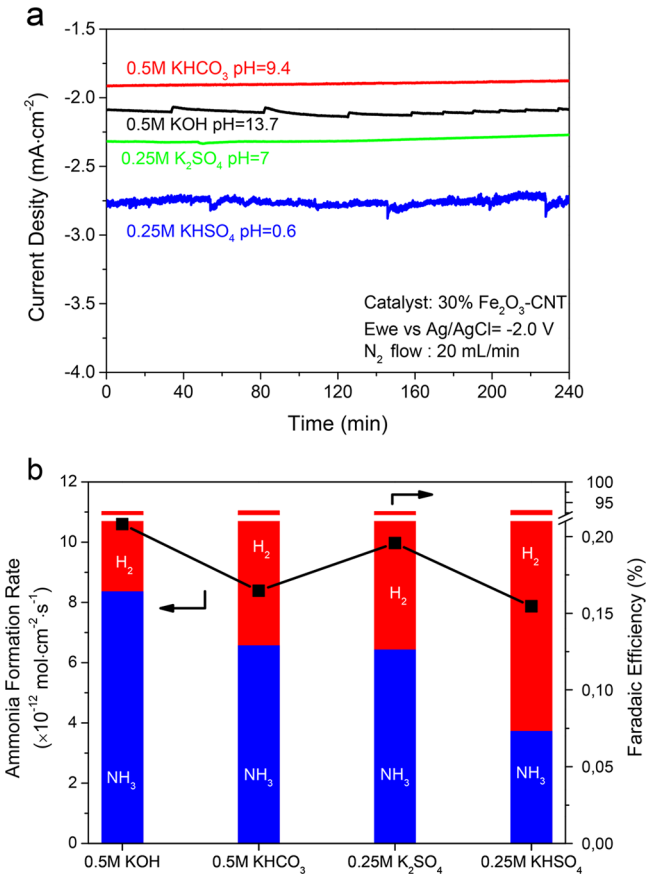

Figure 4. (a) Current density profile of electrocatalyst with different electrolyte; and (b) average ammonia formation rate and Faradaic efficiency of electrocatalyst with different electrolyte.

Note that hydrogen evolution and ammonia formation are the two competitive reactions that took place. For ammonia formation, the overpotential is the dominating factor rather than the mass transfer. However, at the applied voltage −2.0 V vs Ag/AgCl, the mass transport of H^+ is the rate-determining step. Because of the higher Faradaic efficiency (>90%) of hydrogen evolution, the current density is determined by the hydrogen evolution reaction. Therefore, the hydrogen transport rate (depending on the proton concentration and water transport) determines the current density. As a consequence, the current density is determined by the proton concentration when an acid is used as electrolyte.

When a base is used as electrolyte, the water transport directly influences the current density due to the low concentration of protons (<10^{-7} mol/L). The current density thus decreases from −2.09 mA cm^{-2} for 0.5 M KOH (pH = 13.7) to −1.89 mA cm^{-2} for 0.5 M $KHCO_3$ (pH = 9.4) with the water transportation becoming dominant. The difference in current density observed by KOH and $KHCO_3$ is determined by water transportation, because in these base conditions water is the dominant hydrogen source. Note that in the basic condition we assume H_2O reacting with N_2 and e^- to form NH_3 and OH^-. It may be possible that the accumulation of OH^- partly contributes to the deactivation.

In 0.5 M $KHCO_3$ (pH = 9.4), gas bubbles stick on the membrane during the reaction, when $KHCO_3$ was used as electrolyte. We believe that this effect, although not proven in the literature, is related to the generation of CO_2 gas bubbles due to the local change in the pH at the membrane. The presence of bubbles decreases the areas of electrode, so the water transport is hindered. For this reason, current density decreases. A similar effect, but related to the formation of H_2 bubbles, was noted in strong acid conditions. The high level of noise observed in the plots for 0.25 M $KHSO_4$ is related to the hydrogen bubbles, which stick in part to the electrolytes, giving rise to the observed noise of the current density profile. However, it may be noted that, apart from these fluctuations, stable current densities are observed for all electrolytes.

Figure 4b reports a comparison of the ammonia formation rates for the 30% Fe_2O_3-CNT electrocatalyst in the different electrolytes used. The highest ammonia formation rate of 1.06 × 10^{-11} mol cm^{-2} s^{-1} was obtained for the 0.5 M KOH electrolyte, while the lowest rate of 7.87 × 10^{-12} mol cm^{-2} s^{-1} for 0.25 M $KHSO_4$. The total Faradaic efficiency was similar in different electrolytes, with the differences with the experimental error for H_2 detection. However, a significant difference was observed for the Faradaic selectivity to NH_3. The NH_3 Faradaic selectivity of 0.164% obtained by 0.5 M KOH is 225% higher than the value observed by 0.25 M $KHSO_4$.

The experimental observation is thus that the electrolyte (type, pH, concentration) influences significantly the selectivity of NH_3, but has instead a minor effect on the ammonia formation rate. Note, however, that a more detailed interpretation of the effect of the electrolyte requires further in-depth studies, which are out of the scope here. In fact, there are many possible factors to consider in changing the electrolyte, such as that the surface tension changes in different electrolyte solutions and this would impact on the hydrophilicity of the electrode and Nafion membrane. Other relevant aspects are the impact on varying the ohmic contribution through the Nafion membrane, with the influence on varying WE overpotential, etc. Therefore, the electrolyte may influence many aspects, even though it should be remembered that we use here the electrolyte only in the proton generation (water electrolysis) hemicell, while a gas-phase hemicell is present in the NH_3 formation part.

Effect of Applied Voltage. The effect of applied voltage was studied using 2.5 mg/cm^2 of 30% Fe_2O_3-CNT as catalyst, and 0.5 M KOH as electrolyte. Figure 5a reports the current density as a function of time on stream for extended reaction tests (24 h). A quite stable behavior can be observed. Current densities of −0.089, −0.19, and −2.03 mA cm^{-2} were obtained for the applied voltages of −1.0, −1.5, and −2.0 V vs Ag/AgCl, respectively. It is worth pointing out that current density (as an absolute value) for an applied voltage of −1.5 V vs Ag/AgCl is about 2 times higher than the value for an applied voltage of −1.0 V, while the current density registered for an applied voltage of −2.0 V vs Ag/AgCl is about 20 times higher than

DOI: 10.1021/acssuschemeng.7b01742
ACS Sustainable Chem. Eng. 2017, 5, 7393−7400

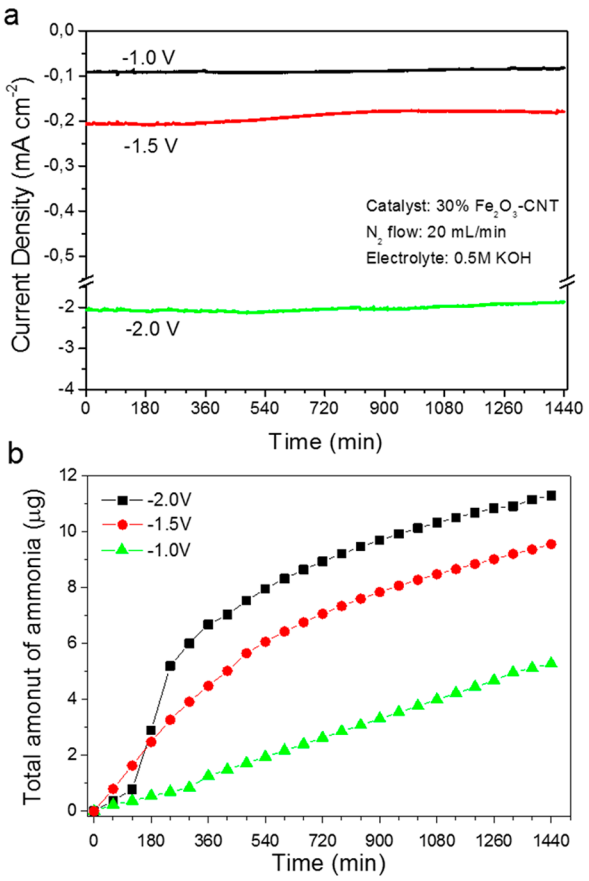

Figure 5. Effect of applied voltage (vs Ag/AgCl) on (a) current density and (b) total ammonia formation.

that for an applied voltage of −1.0 V. A nonlinear increase of the current density by applying higher voltages is thus present. A similar effect was observed on the cumulative (total) amount of ammonia formed (Figure 5b). The final value after 24 h is 5.28, 9.53, and 11.31 μg of ammonia for an applied voltage of −1.0, −1.5, and −2.0 V vs Ag/AgCl, respectively. It may be noted that for the lowest applied voltage (−1.0 V), the rate of ammonia formation (the tangent of the curves reported in Figure 5b) remains constant, whereas the ammonia formation rate decreases with time for the applied voltage of −1.5 V vs Ag/AgCl. For the −2.0 V vs Ag/AgCl applied voltage, the rate of ammonia formation passes instead through a maximum.

To analyze better these aspects, Figure 6 reports the ammonia formation rate (histogram) and NH_3 Faradaic selectivity (average in 60 min time slots) determined for extended-time experiments. As shown in Figure 6a, the highest ammonia formation rate of 1.89×10^{-11} mol cm^{-2} s^{-1} was observed after 4 h in the experiment applying −2.0 V vs Ag/AgCl. The average ammonia formation rate (in 24 h) is about 3×10^{-12} mol cm^{-2} s^{-1}, which is 1.5 times higher than the value when the voltage of −1.0 V vs Ag/AgCl is applied.

As shown in Figure 6b, relative to an applied voltage of −1.5 V vs Ag/AgCl, the best NH_3 Faradaic selectivity of 1.04% was observed in the first 3−4 h. Note that this NH_3 Faradaic selectivity is significantly better than that reported earlier for comparable reaction conditions, for example, by Kordali et al.[8] (a Faradaic efficiency of 0.28%) or Lan and Tao[9] (below 0.1%). The ammonia formation rate maintains over a value of 3×10^{-12} mol cm^{-2} s^{-1} for about 780 min at −1.5 V, while for only 600 min at −2.0 V. At −1.0 V, on the contrary, a lower ammonia formation rate is observed (1.86×10^{-12} mol cm^{-2} s^{-1}), but remains constant in 24 h of experiments. The NH_3 Faradaic selectivity remains also constant (0.59%).

When the voltage of −2.0 V vs Ag/AgCl is applied, the best ammonia formation rate is observed, but with the rate passing through a maximum and showing a relatively fast decrease. When the voltage of −1.5 V vs Ag/AgCl is applied, the best current efficiency is observed, with the rate of ammonia formation also decreasing, but with a lower slope. When a voltage of −1.0 V vs Ag/AgCl is applied, the best stability was observed. Note that instead the current densities (Figure 5a) remain constant during the same period. Therefore, it is not a leaching (no Fe is detected in the electrolyte) or a major change in the electrode, but likely a change in the nature of the iron sites, with a modification from sites active for ammonia synthesis to sites active in H_2 generation, reducing thus the availability of the H^+/e^- for the reduction of N_2. This explains why the current densities remain stable, while a major change in the rate of ammonia formation and Faradaic selectivity is observed. The change in the surface characteristics of iron nanoparticles induced by the applied voltage explains also why the time on stream behavior depends on the applied voltage.

XPS (X-ray photoelectron spectroscopy) ex situ characterization data of the electrode as a function of the time of reaction confirm the change in the nature of the iron species after application of the voltage of −2.0 V vsAg/AgCl. In particular, there is a clear change in the 540−525 eV binding energy region corresponding to the O 1s signal. The fresh sample is characterized by four components, some related to oxygen functional species of carbon (related to carbon oxidative pretreatment) and some related to oxygen species of iron nanoparticles:[13]

- **O1** (Fe−O−Fe, 530.5 eV) related to O^{2-}−Fe_2O_3 or FeOOH species, and **O2** (Fe−O−H, 531.8 eV) related to FeOOH species
- **O3** (C−O−C, 532.4 eV) related to ether functional groups of carbon substrate, and **O4** (C−O−H, 533.8 eV) related to OH or COOH functional groups of carbon substrate

While the latter two O 1s signals (O3 and O4) remain nearly unchanged as a function of the time of application of the voltage of −2.0 V vs Ag/AgCl, a clear change in observed in the O1 and O2 components. In particular, the O3 component increases, while the O4 component initially slightly increases and then decreases following a trend roughly corresponding to that present in the electrocatalytic behavior (Figure 6a). According to these results, the deactivation might be due to the transformation of Fe_2O_3-CNT species to $Fe^{II,III}OH$-CNT during the reaction.

Further studies are in progress to clarify this question, but we can anticipate that preliminary results indicate that the iron particles supported on CNTs should be in an oxidized form, and the formation of metallic Fe leads to a lowering of the Faradaic selectivity due to enhanced rate of H_2 formation. Operando XAFS (X-ray adsorption fine structure) studies in an electrochemical cell adapted to synchrotron light source indicate that, in similar Fe_2O_3/carbon electrodes, a ferrihydrate (FeOOH) structure is present at low negative applied voltages, but by increasing the negative voltage above about −1.3 to −1.4 V vs Ag/AgCl, the formation of an intermediate hydride species appears that discharges as H_2, leaving Fe^0 behind. On increasing the negative applied voltage and time of reaction, the surface of

DOI: 10.1021/acssuschemeng.7b01742
ACS Sustainable Chem. Eng. 2017, 5, 7393−7400

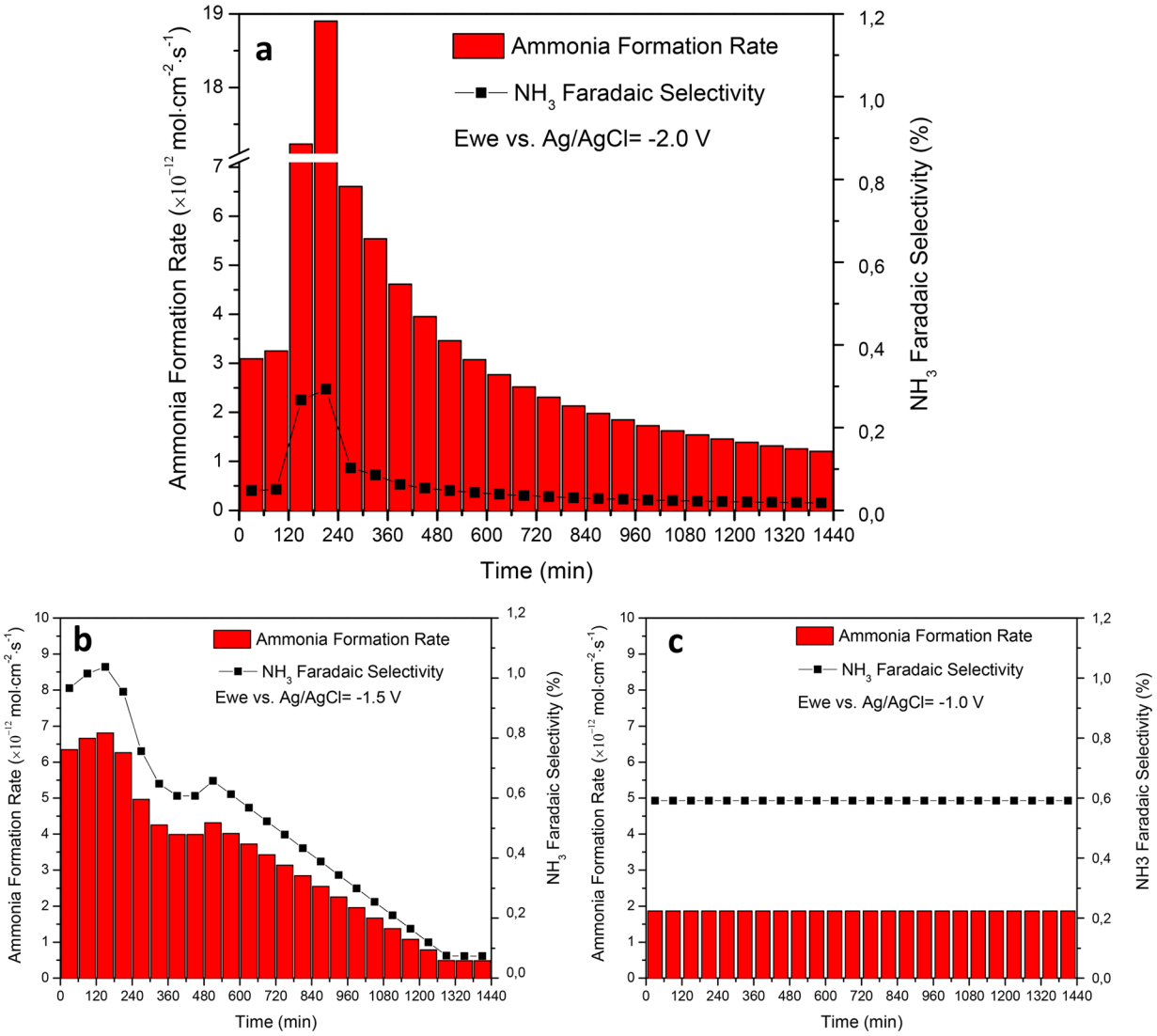

Figure 6. Ammonia formation rate and NH_3 Faradaic selectivity for an applied voltage (vs Ag/AgCl) of (a) −2.0 V, (b) −1.5 V, and (c) −1.0 V.

iron-oxide/hydroxide species starts to be reduced, and this effect leads to enhanced formation of H_2 detrimental for the NH_3 formation.[14]

On the other hand, by application of a higher negative voltage, the driving force for the electron transfer increases and thus the reaction rate. To develop improved Fe/CNT electrocatalysts, it is thus necessary to improve the stability of the iron-oxide particles against the in situ reduction at negative voltages above −1.0 V. At this value, on the contrary, a rather stable activity in ammonia formation is present (Figure 6c), but the rate and Faradaic efficiencies are low.

In conclusion, present data evidence that 30% Fe_2O_3-CNT is the best electrocatalyst among iron-based catalysts supported on carbon nanotubes. The performances greatly depend on the cell design, where the possibility of ammonia crossover through the membrane has to be inhibited. The reaction conditions also play a significant role. When an acid is used as electrolyte, the current density is determined by proton concentration, but if a base is used as electrolyte, the water transport determines the current density. The experimental observation is thus that the electrolyte (type, pH, concentration) influences significantly the selectivity of NH_3, but has instead a minor effect on the ammonia formation rate. The mechanistic interpretation of the effect of the electrolyte requires, however, further in-depth studies. A complex effect of the applied voltage was observed. Excellent stability was found for an applied voltage −1.0 V vs Ag/AgCl. At higher negative applied voltages, the ammonia formation rate and Faradaic selectivity are higher, but with a change of the catalytic performances, although the current densities remain constant for at least 24 h of experiments. This effect is interpreted in terms of reduction of the iron-oxide species above a negative voltage threshold, which enhances the side reaction of H^+/e^- recombination to generate H_2 rather than their use to reduce activated N_2 species, possibly located at the interface between iron-oxide and functionalized CNT.

AUTHOR INFORMATION

Corresponding Authors

*E-mail: schen@unime.it.
*E-mail: perathon@unime.it.

ORCID

Gabriele Centi: 0000-0001-5626-9840

Notes

The authors declare no competing financial interest.

DOI: 10.1021/acssuschemeng.7b01742
ACS Sustainable Chem. Eng. 2017, 5, 7393−7400

■ ACKNOWLEDGMENTS

This work was cofunded through a SINCHEM grant. SINCHEM is a Joint Doctorate program selected under the Erasmus Mundus Action 1 Programme (FPA 2013-0037).

■ REFERENCES

(1) Perathoner, S.; Centi, G. CO_2 recycling: A key strategy to introduce green energy in the chemical production chain. *ChemSusChem* **2014**, *7* (5), 1274−1282.
(2) Jewess, M.; Crabtree, R. H. Electrocatalytic Nitrogen Fixation for Distributed Fertilizer Production? *ACS Sustainable Chem. Eng.* **2016**, *4* (11), 5855−5858.
(3) Kyriakou, V.; Garagounis, I.; Vasileiou, E.; Vourros, A.; Stoukides, M. Progress in the Electrochemical Synthesis of Ammonia. *Catal. Today* **2017**, *286*, 2−13.
(4) Shipman, M. A.; Symes, M. D. Recent progress towards the electrosynthesis of ammonia from sustainable resources. *Catal. Today* **2017**, *286*, 57−68.
(5) Renner, J. N.; Greenlee, L. F.; Herring, A. M.; Ayers, K. E. Electrochemical synthesis of ammonia: a low pressure, low temperature approach. *Electrochem. Soc. Interface* **2015**, *24*, 51−57.
(6) Bao, D.; Zhang, Q.; Meng, F.; Zhong, H.; Shi, M.; Zhang, Y.; Yan, J.; Jiang, Q.; Zhang, X. Electrochemical Reduction of N_2 under Ambient Conditions for Artificial N_2 Fixation and Renewable Energy Storage Using N_2/NH_3 Cycle. *Adv. Mater.* **2017**, *29*, 1604799/1−5.
(7) Shi, M.; Bao, D.; Wulan, B.; Li, Y.; Zhang, Y.; Yan, J.; Jiang, Q. Au Sub-Nanoclusters on TiO_2 toward Highly Efficient and Selective Electrocatalyst for N_2 Conversion to NH_3 at Ambient Conditions. *Adv. Mater.* **2017**, *29*, 1606550/1−6.
(8) Kordali, V.; Kyriacou, G.; Lambrou, Ch. Electrochemical synthesis of ammonia at atmospheric pressure and low temperature in a solid polymer electrolyte cell. *Chem. Commun.* **2000**, *17*, 1673−1674.
(9) Lan, R.; Tao, S. Electrochemical synthesis of ammonia directly from air and water using a $Li^+/H^+/NH_4^+$ mixed conducting electrolyte. *RSC Adv.* **2013**, *3*, 18016−18021.
(10) Chen, S.; Perathoner, S.; Ampelli, C.; Mebrahtu, C.; Su, D.; Centi, G. Electrocatalytic Synthesis of Ammonia at Room Temperature and Atmospheric Pressure from Water and Nitrogen on a Carbon-Nanotube-Based Electrocatalyst. *Angew. Chem., Int. Ed.* **2017**, *56* (10), 2699−2703.
(11) Perathoner, S.; Centi, G.; Su, D. Turning Perspective in Photoelectrocatalytic Cells for Solar Fuels. *ChemSusChem* **2016**, *9* (4), 345−357.
(12) Lan, R.; Irvine, J. T. S.; Tao, S. Synthesis of ammonia directly from air and water at ambient temperature and pressure. *Sci. Rep.* **2013**, DOI: 10.1038/srep01145.
(13) Arrigo, R.; Hävecker, M.; Wrabetz, S.; Blume, R.; Lerch, M.; McGregor, J.; Parrott, E. P. J.; Zeitler, J. A.; Gladden, L. F.; Knop-Gericke, A.; Schlögl, R.; Su, D. S. Tuning the Acid/Base Properties of Nanocarbons by Functionalization via Amination. *J. Am. Chem. Soc.* **2010**, *132*, 9616−9630.
(14) Chiara, C.; Schuster, M.; Gibson, E.; Gianolio, D.; Cibin, G.; Wells, P.; Garai, D.; Solokha, V.; Calderon, S.; Ampelli, C.; Perathoner, S.; Centi, G.; Arrigo, R. Insights by operando XAFS into the high Faraday efficiency and selectivity to acetic acid in the electro-catalytic reduction of CO_2 over FeOOH on N-doped carbon. *Angew. Chemie, Int. Ed.* **2017**, submitted.

DOI: 10.1021/acssuschemeng.7b01742
ACS Sustainable Chem. Eng. 2017, 5, 7393−7400